

# Interacting molecular motors: Efficiency and work fluctuations

František Slanina

*Institute of Physics, Academy of Sciences of the Czech Republic,  
Na Slovance 2, CZ-18221 Praha, Czech Republic \**

(Dated: October 6, 2018)

We investigate the model of “reversible ratchet” with interacting particles, introduced by us earlier [Europhys. Lett. **84**, 50009 (2008)]. We further clarify the effect of efficiency enhancement due to interaction and show that it is of energetic origin, rather than a consequence of reduced fluctuations. We also show complicated structures emerging in the interaction and density dependence of the current and response function. The fluctuation properties of the work and input energy indicate in detail the far-from-equilibrium nature of the dynamics.

PACS numbers: 05.40.-a; 87.16.Nn; 07.10.Cm

## I. INTRODUCTION

Molecular motors [1–10] are subject to intense study both from biological and technological point of view. They are paradigmatic examples of machines operating at nanometer scale. In a cell, motor proteins powered by ATP hydrolysis [11–14] help move molecules to places where they are needed. Motors assist separation of chromosomes, copying DNA into RNA and perform many more functions [15–17]. Technological applications of the underlying mechanisms flourish [18], including e. g. Brownian pumps [19, 20] and quantum tunneling ratchets [21]. They provide also an invaluable testing ground for fundamental questions of transport phenomena far from equilibrium [22].

Many models of molecular motors appeared in the literature since the pioneering work by Ajdari and Prost [23]. The basic mechanism is best elucidated in the models which rely on the ratchet mechanism [4, 5, 24–26] and also bear the name Brownian motors. The basic idea can be viewed either as diffusive motion of a particle in spatially asymmetric time-dependent potential or as chemically driven transitions between a finite number of mechano-chemical states. The former view is more intuitive, but the latter is closer to reality and opens the perspective of fitting the underlying transition probabilities to experimental data.

More realistic models are rather built on Markov chains in the configuration space constructed as product of spatial and internal (chemical) coordinates [8, 27–35]. This approach resides perhaps on more solid experimental evidence, but the absence of explicit potential makes it very difficult to assess the energetic efficiency, the question of principal importance in this paper.

Indeed, one of the points of special interest here will be the question of the efficiency of molecular motors. Several measures of efficiency can be found in literature. We shall use the classical thermodynamic definition  $\eta = W/E_{\text{in}}$ , where  $W$  is work performed and  $E_{\text{in}}$  energy supplied to

the system from external source. Alternative measure takes into account viscous resistance [36], thus reflecting better the reality, at the cost that the inequality  $\eta < 1$  is not guaranteed automatically. Yet other methods of measuring the efficiency involve explicitly the consumption of chemical energy [37], or the magnitude of the stopping force [9]. Note, however, that the former work ([37]) explores the interacting motors and the mechanism if generating the non-zero current is related to spontaneous symmetry breaking and this it is principally different from the non-interacting case studied in [9]. Therefore, the direct comparison of the efficiency in these two cases is hardly possible. We are not aware of any work in which several measures of efficiency would be systematically compared on the same model.

The efficiency of canonical Brownian motors realized as either flashing or rocking ratchets was intensely studied [27–29, 38–43]. It turns out that the energetic efficiency is rather low [5, 41], while the experimental data on motor proteins, e. g. the kinesin [9, 11], report high efficiency, sometimes even estimated to be close to 100 per cent. We are not in a position to judge the quantitative precision of these empirical estimates, although it can be suspected that the error margin is rather high. However, one is lead to a natural conclusion that the usual ratchet mechanism with diffusion as principal driving force is not an appropriate model for biological motors.

In idealized case we can distinguish between ratchet and power-stroke mechanisms for molecular motors [44], the latter relying rather on quasi-deterministic downhill motion in a free-energy landscape which evolves in time. Thus, the particles move as if trapped in a traveling potential wave. This idea was elaborated in a toy model of “reversible ratchet” [43, 45, 46], showing much higher efficiency, close to the biologically relevant figures. Of course, arbitrary combinations and mixtures of the ratchet and power-stroke mechanisms can be invented and indeed, they are believed to be found in reality, e. g. in the myosin V motor (see the review [35] and references therein). Nevertheless, it is useful to compare these two extremes. We should also note that high efficiency was characteristic of the models of either interacting [37] or non-interacting [47, 48] motors, which do combine the

---

\*Electronic address: slanina@fzu.cz

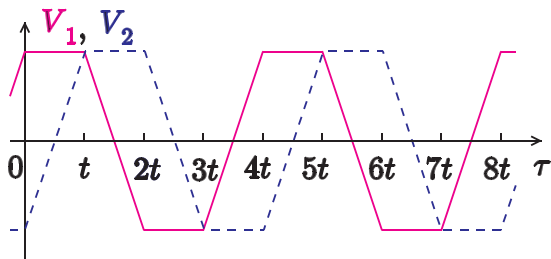


FIG. 1: (Color online) Graph of the time dependence of the potential in which the particles move. Full line:  $V_1(\tau)$ , dashed line:  $V_2(\tau)$ . The potential at the third site,  $V_0$ , is time independent.

ratchet and power-stroke mechanisms.

The second point we shall concentrate on in this work will be the mutual repulsive interaction of molecular motors. In the cell, the steric (hard-core) repulsion of motor proteins influences significantly their behavior. For example, in gene transcription and translation large number of motor proteins move along the same track [15, 16], forming the so-called “Christmas tree” structures. Thus, they show themselves as a physical realization of the well-studied asymmetric exclusion process, introduced first in the context of biopolymerization [49, 50] and later solved exactly in great detail, using sophisticated techniques [22, 51–53]. The model was adapted for molecular motors, which may attach and detach with defined rates [54, 55]. Later, this situation was studied theoretically for the cases of kinesin [56], ribosomes [57], and RNA polymerase [58], using the procedures developed in traffic models [59]. The influence of the geometry of the compartment in which the interacting motors diffuse after detachment from the track was studied e. g. in [60].

Interaction of motors brings about even more complicated collective effects. In the cell, kinesin and dynein molecules typically carry the cargo in groups [8, 9, 61], resulting in current reversals. Including explicitly the ratchet mechanism of driven diffusion of hard-rod particles leads to very intricate effects [62–64], if the particle size and the ratchet periodicity are incommensurate. The collective movement of coupled Brownian motors was studied [65–68] and in some cases the coupling was found to induce non-zero current and spontaneous oscillations even in mirror symmetric potential due to dynamical symmetry breaking [37, 69]. In analogy with these works, the motion of a few rigidly bound motors was studied [70]. A special case of such interaction is the coordination of the two motor heads within single kinesin molecule, which leads also to non-trivial effects [34]. Finally, let us mention the interaction of the motors with the track, studied in “burnt-bridge” models, e. g. in Ref. [71].

In our previous paper [72] we introduced a model, which is a modified version of the “reversible ratchet”. Spatial coordinate is discretized, as e. g. in [26]. Tun-

able on-site repulsion between particles is introduced. We found in [72] that not too strong interaction leads to increase of efficiency. This effect was reproduced qualitatively in analytical calculations based on mean-field (MF) approximation. Quantitative agreement was reached in an improved MF treatment, developed in [73]. Here we investigate the model in depth by further numerical simulations. Especially, we elucidate the origins of the interaction-enhanced efficiency. We shall show that it stems from the energy balance rather than from suppression of fluctuations. At stronger interaction and/or higher density, current reversals and oscillations in response function are found. We also calculate the distribution of input energy and performed work, which is far from being Gaussian.

## II. REVERSIBLE RATCHET WITH INTERACTING PARTICLES

Our model contains  $N$  particles occupying integer positions on a segment of length  $L$ , with periodic boundary conditions, and evolves in discrete time. The position of  $i$ -th particle at the instant  $\tau$  is denoted  $x_i(\tau)$ . The particles move under the influence of a variable driving force with spatial period 3 and temporal period  $4t$ . The potential of this force is  $V(x, \tau) = V(x, \tau + 4t) \equiv V_{x \bmod 3}(\tau)$ , at site  $x$  and time  $\tau$ . The three independent values of the potential  $V_a(\tau)$ ,  $a = 0, 1, 2$  evolve in a four-stroke pattern, with  $V_0(\tau) = 0$  and the remaining two being delayed one with respect to the other by one quarter-period  $t$ . Thus, we prescribe

$$V_1(\tau) = V_2(\tau + t) = \begin{cases} V & \text{for } 0 < \tau < t \\ V + 2V(1 - \tau/t) & \text{for } t < \tau < 2t \\ -V & \text{for } 2t < \tau < 3t \\ -V - 2V(1 - \tau/t) & \text{for } 3t < \tau < 4t. \end{cases} \quad (1)$$

We easily recognize the traveling-wave character of this potential, corresponding to the power-stroke mechanism of the molecular-motor movement. In all the rest of this paper, we fix the amplitude of the potential  $V = 1$ . The time dependence of the potential is illustrated in Fig. 1.

Besides the driving potential, there is also a uniform external force from the useful load  $F$  and, most importantly, the repulsive interaction from other particles. We suppose the interaction is on-site only and we tune its strength, in order to interpolate between the non-interacting and hard-core cases. The  $j$ -th particle feels the potential from all remaining ones. To formalize it, we denote  $n_j(x, \tau) = \sum_{i=1}^N \bar{\delta}(i-j)\delta(x-x_i(\tau))$  the number of particles, except  $j$ -th particle, at site  $x$ . (We use  $\delta(a-b)$  for Kronecker delta and  $\bar{\delta}(a-b) = 1 - \delta(a-b)$ .) Thus, the  $j$ -th particle moves in the potential

$$U_j(x, \tau) = V(x, \tau) + xF + \frac{g}{1-g} n_j(x, \tau). \quad (2)$$

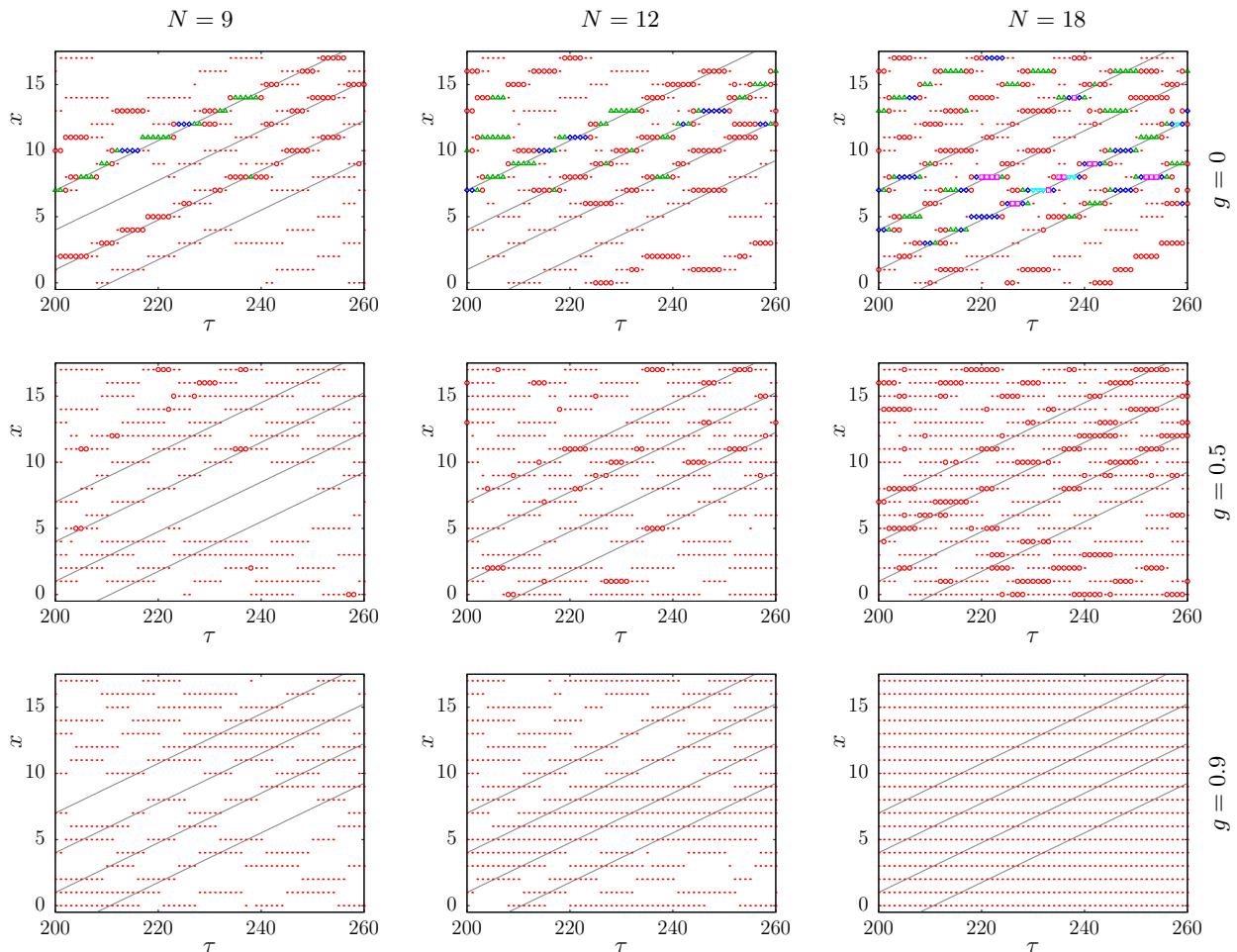


FIG. 2: (Color online) Spatio-temporal diagrams of the configurations of the motor particles. The width of the sample is  $L = 18$ , temperature  $T = 10$ , quarter-period  $t = 4$ , external load  $F = 0$ . Each panel corresponds to different combination of two parameters, the number of particles  $N$  and the interaction strength  $g$ , whose values are indicated at corresponding columns and rows. Dots denote presence of exactly one particle at given space and time, the other symbols presence of more particles, namely two ( $\circ$ ), three ( $\triangle$ ), four ( $\diamond$ ), five ( $\square$ ), and six ( $\nabla$ ). The diagonal straight lines are guides for the eye, indicating the movement of the minima of the potential  $V(x, \tau)$ .

For  $g = 0$  we recover the non-interacting case, while when  $g \rightarrow 1$  we approach the hard-core interaction of the exclusion process [22]. In contrast with the previous work [72], we use here different form of the interaction in order to see the limit of hard-core repulsion when  $g \rightarrow 1$ . Although it may cause some small difficulties when comparing the results of [72] with the present ones, the advantage lies in the possibility to see the transition from non-interacting case to hard-core repulsion on a finite interval  $g \in [0, 1]$ .

The simulation algorithm proceeds as follows. At each integer time  $\tau$  we instantly shift the potential according to (1). Then, we choose  $N$  times a particle randomly and let it try to make a jump. Therefore, on average every particle makes one attempt per one time unit, but the probability that a given particle performs actually  $k$  attempts approaches Poisson distribution with unit mean,  $P(k) = 1/(e k!)$ , when  $N$  is large. For small  $N$  there

is a deviation from the Poisson distribution, which induces slight finite-size effects, but in [72] we showed that they can be neglected for  $N$  larger than about 100. Note that in each of these  $N$  attempts the external potential  $V(x, \tau)$  is the same, but the potential  $U_j(x, \tau)$  felt by the particle  $j$  may change, because the configuration of particles  $n_j(x, \tau)$  changes after each particle jump.

In one attempt, the particle is allowed to jump one site to the right or left. The probability of the jump  $x \rightarrow y$  of the  $j$ -th particle is

$$W_{j,x \rightarrow y} = \frac{1}{2} \left( 1 + e^{\beta (U_j(y, \tau) - U_j(x, \tau))} \right)^{-1} \quad (3)$$

if  $|x - y| = 1$  and zero if  $|x - y| > 1$ . For convenience, we define the temperature  $T$  so that  $\beta = 270/T$ .

Let us now specify the main measurables. The simplest

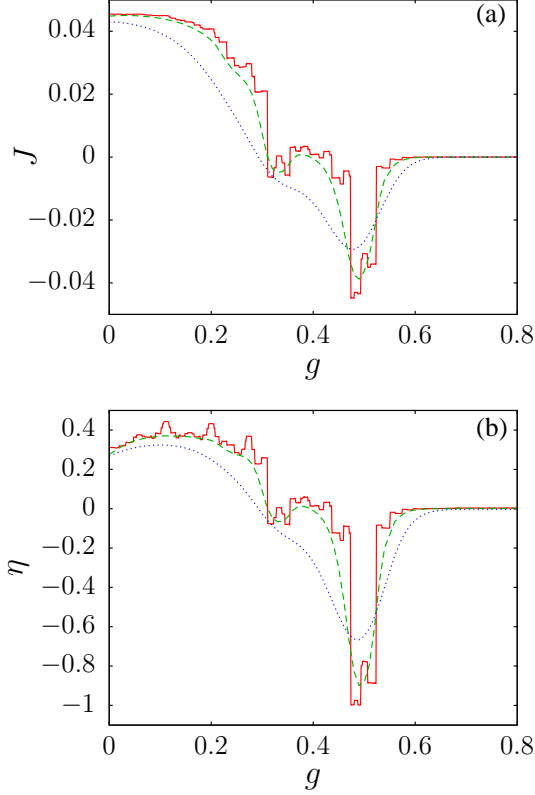


FIG. 3: (Color online) Current (panel (a)) and efficiency (panel (b)) as a function of interaction strength, for  $N = L = 1200$ ,  $t = 16$ , and  $F = 0.1$ . The temperature is  $T = 0$  (solid line),  $T = 10$  (dashed line), and  $T = 30$  (dotted line).

quantity of interest is the current

$$J(\tau) = \sum_i (x_i(\tau+1) - x_i(\tau)) \quad (4)$$

or rather its time average per particle  $J = \lim_{\tau \rightarrow \infty} (\tau N)^{-1} \sum_{\tau'=1}^{\tau} J(\tau')$ . As we are interested in the energetics of the motor, we must define the energy input and the useful work done by the particle. The latter quantity, at time  $\tau$ , is simply  $w(\tau) = F J(\tau)$ . The energy pumped into the motor from outside relates to the change of the potential  $V_a(\tau)$  while the particles stay immobile. Thus, the energy absorbed by the particle  $i$  between steps  $\tau - 1$  and  $\tau$  is

$$a_i(\tau) = V(x_i(\tau), \tau) - V(x_i(\tau), \tau - 1) \quad (5)$$

and the efficiency, accordingly,

$$\eta = \lim_{\tau \rightarrow \infty} \frac{\sum_{\tau'=1}^{\tau} w(\tau')}{\sum_{\tau'=1}^{\tau} \sum_i a_i(\tau')} \quad (6)$$

Later in this paper we shall investigate the distribution of the particle shift

$$P(\Delta x) = \frac{1}{\mathcal{N}} \sum_{\tau} \sum_i \delta(x_i(\tau + \Delta\tau) - x_i(\tau) - \Delta x) \quad (7)$$

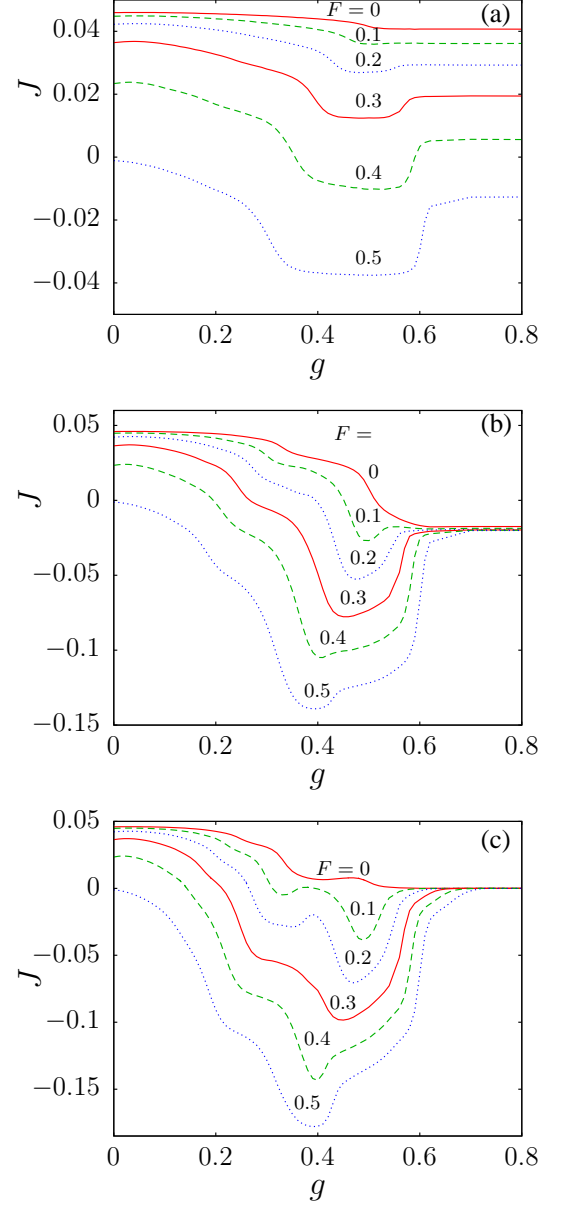


FIG. 4: (Color online) Current as a function of interaction strength, for  $L = 1200$ ,  $t = 16$ , and  $T = 10$ . The number of particles is  $N = 360$  (density  $\rho = 0.3$ ) in the panel (a),  $N = 840$  (density  $\rho = 0.7$ ) in the panel (b), and  $N = 1200$  (density  $\rho = 1$ ) in the panel (c). Different curves correspond to load, from top to bottom,  $F = 0$  (solid), 0.1 (dashed), 0.2 (dotted), 0.3 (solid), 0.4 (dashed), 0.5 (dotted).

and also the joint distribution with the input energy

$$\begin{aligned} P(E_{\text{in}}, \Delta x) &= \\ &= \frac{1}{\mathcal{N}} \sum_{\tau} \sum_i \delta\left(\sum_{\tau'=\tau+1}^{\tau+\Delta\tau} a_i(\tau') - E_{\text{in}}\right) \times \\ &\quad \times \delta(x_i(\tau + \Delta\tau) - x_i(\tau) - \Delta x) \end{aligned} \quad (8)$$

where  $\mathcal{N}$  is the appropriate normalization. Note that

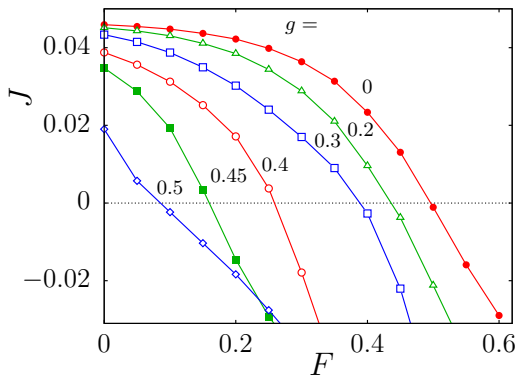


FIG. 5: (Color online) Dependence of the current on the load, for  $L = 1200$ ,  $N = 600$ ,  $T = 10$ ,  $t = 16$  and interaction  $g = 0$  ( $\bullet$ ),  $0.2$  ( $\triangle$ ),  $0.3$  ( $\square$ ),  $0.4$  ( $\circ$ ),  $0.45$  ( $\blacksquare$ ),  $0.5$  ( $\diamond$ ).

in both distributions there is implicit dependence on the time lag  $\Delta\tau$ .

### III. ENHANCED EFFICIENCY

We show in Fig. 2 examples of typical evolutions of the particle configurations, for three densities ( $\rho = 1/2$ ,  $\rho = 2/3$ , and  $\rho = 1$ ) and three interaction strengths ( $g = 0$ ,  $g = 0.5$ , and  $g = 0.9$ ). We can see that without interaction, particles are bunched together and dragged by the traveling wave of the periodic potential. Interaction smears out this picture, suppresses the current and makes at the same time the local particle density more uniform.

The typical dependence of the current and efficiency on the interaction strength is shown in Fig. 3. At zero temperature, the dependence contains many steep steps with multiple maxima and minima. Therefore, for some values of the external load  $F$  the current changes sign several times when the interaction increases. For larger temperatures there are still visible traces of this complex dependence, although the singularities (sharp steps) are smeared out. We also observe that both the current and efficiency approaches zero for very strong repulsion ( $g \rightarrow 1$ ). We shall see later that this feature is special to some values of the particle density  $\rho = N/L$ , for example to  $\rho = 1$ , which applies to Fig. 3. The generic feature is that for interaction above about  $g \simeq 0.6$  the current and efficiency approach a constant value.

The most important finding, from the point of view of practical use of the motors, is the increase of the efficiency when the interaction is switched on but is not too strong. For zero temperature we observe multiple maxima of the efficiency, which transform into a unique maximum at higher temperatures. The effect of efficiency enhancement was investigated in detail in our previous work [72]. In this paper we return to the origin of this effect later, when we shall discuss the energy balance and

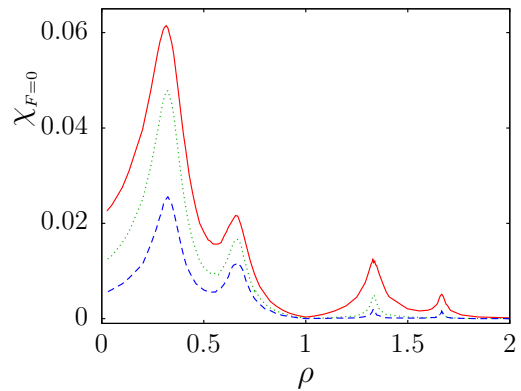


FIG. 6: (Color online) Dependence of the response at zero load on particle density, for  $N = 1200$ ,  $t = 16$ ,  $g = 0.9$  and the temperature  $T = 30$  (solid line),  $T = 10$  (dotted line), and  $T = 0$  (dashed line).

work fluctuations.

In Fig. 4 we can see three sets of results for the current, differing in the density of particles. Different curves in one set correspond to different external load  $F$ . All three cases (and also the data shown in Fig. 3) exhibit minimum current, i. e. smallest effective driving, at interactions somewhere around  $g \simeq 0.4$  to  $g \simeq 0.5$ . In order to see what is special in this value of the interaction, we should note that the change of the potential due to presence of a single particle  $g/(1-g)$  is equal to the amplitude of the traveling-wave potential  $V = 1$  just for  $g = 0.5$ . At this value of the interaction, one particle may block, or at least significantly hinder, the movement of the remaining particles.

We can see that for low density,  $\rho < 0.5$ , the asymptotic current for strongly interacting particles,  $g \rightarrow 1$ , is positive at low load and at the same time is sensitive to the value of the load. On the other hand, for  $0.5 < \rho < 1$  the asymptotic current at zero load is negative, i. e. the interaction induces current reversal. Contrary to the previous case, the asymptotic current seems to be extremely weakly dependent on the load. The third panel shows again that the asymptotic current is zero for unit density, independently of the load.

Complementary information can be read from Fig. 5, showing the dependence of the current on the load. We can observe, how the current decreases with the interaction in the full range of observed  $F$ . As a consequence, also the stopping force, i. e. the value of  $F$  for which  $J = 0$ , decreases with increasing interaction. It is also interesting to note the non-linear decrease of the current with the load. So, the response function, defined as the derivative  $dJ/dF$ , depends on  $F$ .

In Fig. 6 we can see how the zero-load response function

$$\chi_{F=0} = - \lim_{F \rightarrow 0} \frac{dJ}{dF} \quad (9)$$

depends on the density, in the regime of very strong

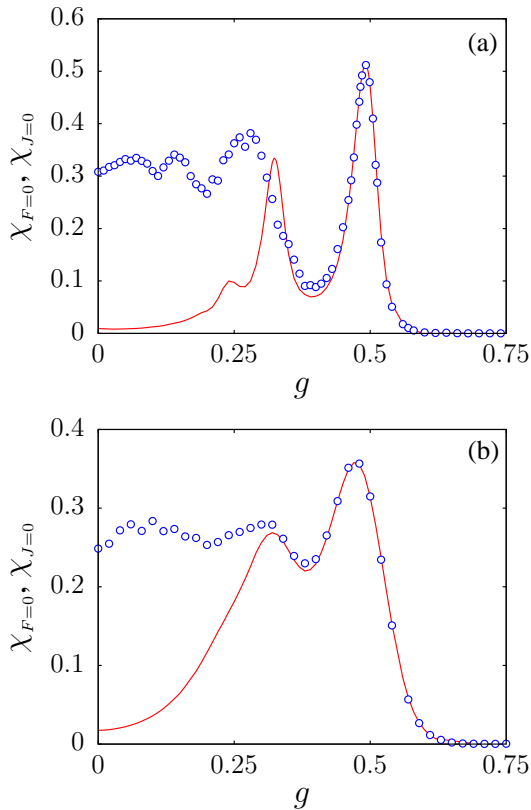


FIG. 7: (Color online) Dependence of the response on interaction strength, for  $L = N = 1200$ , and  $t = 16$ . Lines: response at zero load; symbols: response at zero current. The temperature is  $T = 10$  (panel (a)),  $T = 30$  (panel (b)).

but finite repulsion ( $g = 0.9$ ). Globally, the response is stronger at higher temperature, which is due to the fact that at low temperature the movement of the particles is determined to larger extent by the traveling wave, with lesser influence of the external load, provided the load is small. An interesting feature is the structure of the peaks and the minima seen in Fig. 6 at all temperatures. At integer values of the density the response approaches zero. The other minima are not so deep and are located at densities slightly above the values  $\rho = 1/2$ ,  $\rho = 3/2$  etc. Interestingly, the maxima are found at densities very close to the fractions  $\rho = 1/3$ ,  $\rho = 2/3$ ,  $\rho = 4/3$ , and  $\rho = 5/3$ .

As we already said, the response depends on the load, so we must distinguish from  $\chi_{F=0}$  at least one more response function, defined at zero current

$$\chi_{J=0} = - \left( \lim_{J \rightarrow 0} \frac{dF}{dJ} \right)^{-1}. \quad (10)$$

We can compare these two quantities in Fig. 7. The difference between  $\chi_{F=0}$  and  $\chi_{J=0}$  is especially marked for low interaction strength, while at about  $g \simeq 0.3$  they come close to each other and at  $g \simeq 0.5$  the two become nearly indistinguishable. The source of this behavior can be understood looking at Fig. 5. Without interaction,

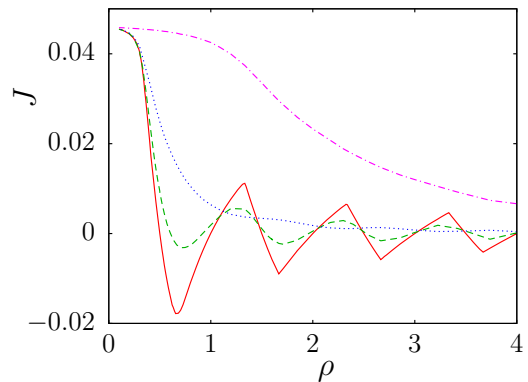


FIG. 8: (Color online) Dependence of the current on particle density, for  $N = 1200$ ,  $T = 10$ ,  $t = 16$ ,  $F = 0$  and interaction  $g = 0.9$  (solid line),  $g = 0.52$  (dashed line),  $g = 0.49$  (dotted line), and  $g = 0.3$  (dash-dotted line).

the dependence of the current on the external load is markedly non-linear, so that the derivative at  $F = 0$  and  $J = 0$  differ. Increasing the interaction, the non-linearity weakens and at  $g \simeq 0.5$  we observe nearly linear dependence, resulting in nearly equal values of the derivative at  $F = 0$  and  $J = 0$ . Note that the density is  $\rho = 1$  in Fig. 7 and both response functions approach zero when  $g \rightarrow 1$ , in accordance with the results shown in Fig. 6.

It is interesting that the dependence on  $g$  exhibits several peaks. The last (and highest) one is located at  $g = 1/2$  and has nearly the same shape both in  $\chi_{F=0}$  and  $\chi_{J=0}$ . However, at lower  $g$  the peaks in the two response functions are much different. We already mentioned that the interaction  $g = 1/2$  is special, as the change in potential due to presence of a single particle just equals the amplitude of the periodic potential  $V(x)$ . Also the second highest peak in  $\chi_{F=0}$  seems to be located at a special value of the interaction strength, namely close to  $g = 1/3$ . We can also see a small peak close to  $g = 1/4$ . We believe these special values are due to special blocking configurations of particles, which enhance the sensitivity of the system to the presence of the external load. Indeed,  $g = 1/3$  means that two particles on the same site contribute as much as the amplitude of  $V(x)$ , at  $g = 1/4$  the same holds for three particles at a site.

To avoid confusion, we do not claim that the configurations of one, two, three, etc. particles are more (or less) frequent at certain values of  $g$ . What we claim is the following. These configurations happen time to time. When they do happen, and if  $g$  has special values, they cause large sensitivity to the value of the load. For other values of  $g$ , the sensitivity to the load is weaker, whatever configuration of particles occurs.

We also looked at the density dependence of the current at high density and strong interaction. The results are summarized in Fig. 8. For the strongest interaction investigated,  $g = 0.9$ , the curve  $J(\rho)$  has a very peculiar zig-zag shape, with zeros at  $\rho = m/2$ , maxima at



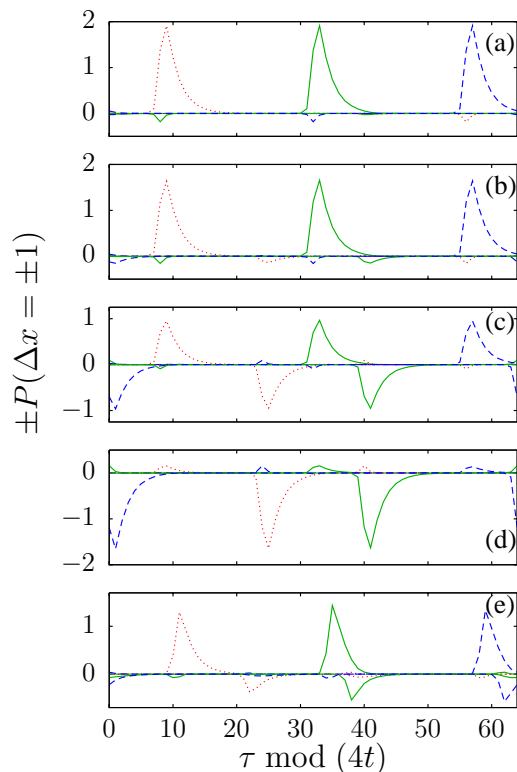


FIG. 9: (Color online) The weight of forward (positive quantities) and minus weight of backward (negative quantities) steps performed at instants  $\tau' = \tau \bmod (4t)$  within the period. The steps originate at points  $x' = x \bmod 3$ , where  $x' = 0$  corresponds to dotted line,  $x' = 1$  to solid line, and  $x' = 2$  to dashed line. The five panels have the following parameters, starting from the top. (a):  $N = 400$ ,  $g = 0$ ,  $F = 0$ . (b):  $N = 400$ ,  $g = 0.9$ ,  $F = 0$ . (c):  $N = 600$ ,  $g = 0.9$ ,  $F = 0$ . (d):  $N = 800$ ,  $g = 0.9$ ,  $F = 0$ . (e):  $N = 400$ ,  $g = 0.9$ ,  $F = 0.3$ . All five:  $L = 1200$ ,  $T = 10$ ,  $t = 16$ .

$\rho = m + 1/3$ , and minima at  $\rho = m - 1/3$ , for positive integer  $m$ . When the interaction is weakened, the sharp cusps become mild waves, until the structure of maxima and minima vanishes at about  $g = 0.5$ . For smaller  $g$ , the current is a monotonously decreasing function of density.

Note that the motor with hard-core repulsion undergoes a current reversal at a density within the interval  $\rho \in (0, 1)$ . This is in sharp contrast with the asymmetric exclusion process, where the current is proportional to  $\rho(1 - \rho)$ . The reason for this difference lies in rather different way the particles are driven. In ASEP, there is constant and homogeneous drift, only hindered by the exclusion principle. In our model, the driving originates from the time dependence of the potential, therefore, it is also space- and time-dependent. The orientation of the current depends on precise timing of the potential changes at different places. The interaction changes the potential a particle feels and the current is susceptible to the details of the potential, so there is no guarantee that the orientation of the current will be the same with inter-

action as it was without interaction. Indeed, the current reversal phenomenon demonstrates that the orientation of the current does change due to the interaction. Note also that the current reversal was observed (qualitatively correctly) also in the approximate mean-field calculation [73].

Some insight into the current reversal phenomenon can be gained from the statistics of forward and backward steps at different places and different times within the period. We define the measured weight  $P(\Delta x = \pm 1; x', \tau')$  as the average number of particles which jump forward (“+” sign) and backward (“-” sign) from site  $x$  at time  $\tau$ , where  $x' = x \bmod 3$  and  $\tau' = \tau \bmod (4t)$ . Note that it is not a probability, because it is not normalized to unity. We can see a typical example in Fig. 9. We can see that without interaction the particles alternately prefer to jump forward from sites  $x' = 0, 1$ , and  $2$ . The backward jumps are rare. This behavior is independent of the particle density by definition. If we add strong repulsion,  $g = 0.9$ , the picture differs substantially in the low and high density regime. For  $\rho = 1/3$  the statistics of forward jumps differs little from the non-interacting case, and the frequency of backward jumps is increased, but remains low. At half filling,  $\rho = 1/2$ , the particles jump alternately forward and backward, at different times, so that the total effect is zero current, as seen already in Fig. 8. When the density is further increased to  $\rho = 2/3$ , the statistics is nearly a mirror image of the case  $\rho = 1/3$ . The particles preferably jump backward at specific places and times, and the forward jumps are rare. For comparison, we show in the last panel of Fig. 9 how the statistics is influenced by non-zero external load. The time dependence looks similar, but weight of forward jumps is suppressed and the weight of backward ones is enhanced.

As the probability of the jumps reflects the local potential, and therefore the local instantaneous configuration of particles, through the formula (3), the statistics of the jumps shown in Fig. 9 tells us, what is, on average, the local neighborhood of a particle at positions  $x'$  and times  $\tau'$ . Change in the shape of the jump statistics reflects the reorganization of the local particle configurations due to repulsive interaction. We can clearly see that the reorganization of the particles can be so dramatic that the current changes sign.

For comparison, we show also the statistics of jumps in the presence of non-zero external load. The suppression of positive and enhancement of negative peaks is visible, as expected.

Similar analysis can also make more clear the argument stated before, that the peaks in the response function at special values of  $g$  are related to the enhanced sensitivity of certain configurations of particles to external load. For example, for  $g = 0.5$  such sensitive situation occurs when a particle tries to hop to a site where there is already a single particle. To support this view we plot a similar statistics as in Fig. 9, but for the difference in the count for force  $F = 0.01$  and opposite  $F = -0.01$ , on condition

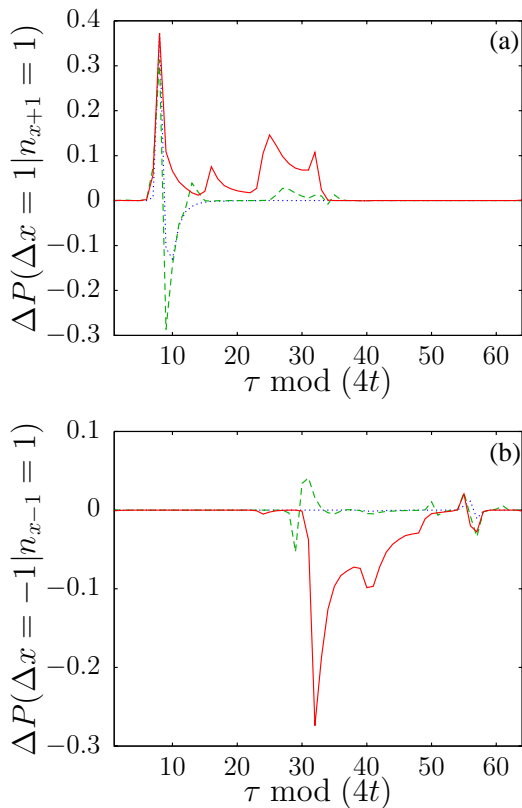


FIG. 10: (Color online) Sensitivity of the weight of forward (a) and backward (b) steps to the change in external load. In this statistics, steps originate at site  $x$ , where  $0 = x \bmod 3$  and particles go to the site already occupied by exactly one particle. Solid line corresponds to interaction  $g = 0.5$ , dashed line  $g = 0.4$ , dotted line  $g = 0$ . Other parameters are  $N = L = 1200$ ,  $T = 10$ ,  $t = 16$ . As for the external load  $F$ , see the definition of the plotted quantities in the main text.

that the site to which the particle is moving, already contains exactly one other particle. We can write that quantity as

$$\begin{aligned} \Delta P(\Delta x = \pm 1 | n_{x\pm 1} = 1) &\equiv \\ &\equiv P(\Delta x = \pm 1 | n_{x\pm 1} = 1) \Big|_{F=-0.01} - \\ &- P(\Delta x = \pm 1 | n_{x\pm 1} = 1) \Big|_{F=0.01} \end{aligned} \quad (11)$$

where  $x$  is the original position of the particle,  $x \pm 1$  the position after the move,  $n_{x\pm 1}$  number of other particles at the site where the particle is about to move. We plot an example of this statistics in Fig. 10. We compare the situation at interaction  $g = 0$ ,  $g = 0.4$ , and  $g = 0.5$ . We can see that the case  $g = 0.5$  is indeed special. The sensitivity to the external load is larger. Moreover, the difference in statistics has the same sign for almost all instants within the time period (positive for forward moves, negative for backward ones), while both for  $g = 0$  and  $g = 0.4$  there are positive as well as negative differences.

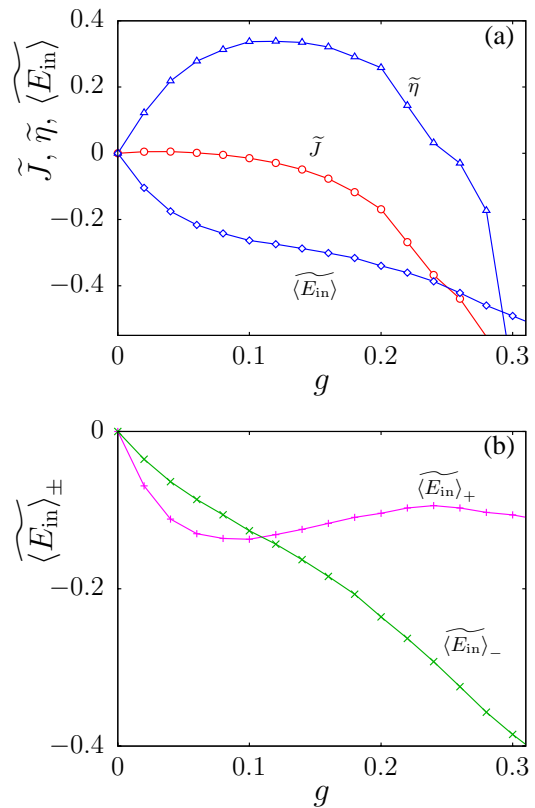


FIG. 11: (Color online) Current ( $\circ$ ), efficiency ( $\triangle$ ), average energy input ( $\diamond$ ) and its positive (+) and negative ( $\times$ ) parts, all relative to the value at  $g = 0$ . The other parameters are  $N = L = 1200$ ,  $T = 10$ ,  $t = 16$ , and  $F = 0.1$ .

#### IV. WORK FLUCTUATIONS

To understand better the effect of enhanced efficiency due to interaction, we shall look at the energy balance and fluctuations. First, we compare the values of current, efficiency and average input energy  $\langle E_{\text{in}} \rangle$  relative to their values at zero interaction, denoted  $J_0$ ,  $\eta_0$ , and  $\langle E_{\text{in}} \rangle_0$ , respectively. More precisely, we plot the typical interaction dependence of the quantities  $\tilde{J} = J/J_0 - 1$ ,  $\tilde{\eta} = \eta/\eta_0 - 1$  and  $\widetilde{\langle E_{\text{in}} \rangle} = \langle E_{\text{in}} \rangle / \langle E_{\text{in}} \rangle_0 - 1$  in Fig. 11. We can clearly see that the initial increase of efficiency for small  $g$  is accompanied by nearly no change in the current, while the input energy decreases. Therefore, the enhanced efficiency is due to lower energy input, while the output (the work) remains nearly unchanged. When the interaction strength increases further, the current starts decreasing as well and so does the work, which is proportional to  $J$ . This effect finally outweighs the lower energy input and the efficiency decreases again. This is the source of the maximum in the efficiency at moderate values of the interaction.

We can get a bit more detailed information if we split the input energy into its positive and negative parts. Recall, that according to the definition (8) the input energy



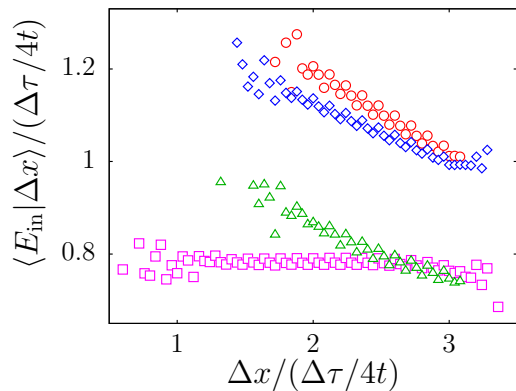


FIG. 12: (Color online) Dependence of the average energy input gained by one particle on the shift of the particle. The quarter-period is  $t = 16$  and the time lag  $\Delta\tau = 100t$  (i. e. 25 periods). The temperature is  $T = 10$  ( $\circ$  and  $\triangle$ ),  $T = 30$  ( $\square$  and  $\diamond$ ). The interaction is  $g = 0$  ( $\circ$  and  $\diamond$ ),  $g = 0.1$  ( $\square$  and  $\triangle$ ). The remaining parameters are  $N = L = 1200$ ,  $F = 0.1$ . The horizontal axis is normalized by the number of time periods, which is  $\Delta\tau/4t$ , therefore it expresses the shift per period.

is  $E_{\text{in}} = \sum_{\tau'=\tau+1}^{\tau+\Delta\tau} a_i(\tau')$ . We separate the contributions from times when  $a_i(\tau')$  is positive from those when it is negative. The former correspond to the shift of the potential  $V(x, \tau)$  upward, that latter to its downward move. So,  $E_{\text{in}\pm} = \sum_{\tau'=\tau+1}^{\tau+\Delta\tau} \pm a_i(\tau') \theta(\pm a_i(\tau'))$ , where  $\theta(x)$  is the Heaviside function. With this definition we have  $E_{\text{in}} = E_{\text{in}+} - E_{\text{in}-}$ . We then define the contributions from positive and negative potential moves to the quantity  $\langle E_{\text{in}} \rangle$  as  $\langle E_{\text{in}} \rangle_+ = (\langle E_{\text{in}+} \rangle - \langle E_{\text{in}+} \rangle_0) / \langle E_{\text{in}} \rangle_0$  and  $\langle E_{\text{in}} \rangle_- = (\langle E_{\text{in}-} \rangle_0 - \langle E_{\text{in}-} \rangle) / \langle E_{\text{in}} \rangle_0$  where, as above, the subscript 0 denotes the quantities computed at  $g = 0$ . Hence  $\langle E_{\text{in}} \rangle = \langle E_{\text{in}} \rangle_+ + \langle E_{\text{in}} \rangle_-$ . We show the dependence of  $\langle E_{\text{in}} \rangle_{\pm}$  again in Fig. 11. We can see that both positive and negative parts contribute to the decrease of the input energy. The contribution of the positive part is larger in the most interesting region of moderate  $g$ , where the efficiency grows with interaction, while for larger  $g$  the decrease of the negative part becomes more important. This leads to the following explanation of the effect of increased efficiency.

At not too high temperature, the particles are chiefly driven by the traveling wave of the periodic potential. This is the power-stroke mechanism of the molecular motor. When the interaction is switched on, but remains small, the particles move in an effective potential which differ little from the original traveling wave. So, the current remains nearly the same, as testified in Fig. 11, while the input energy is lowered, as is also seen in Fig. 11. This lowering could be understood as follows. On the other hand, the repulsion affects the distribution of particles within the period of the potential  $V(x)$ . The minima become shallower, therefore the particles are less

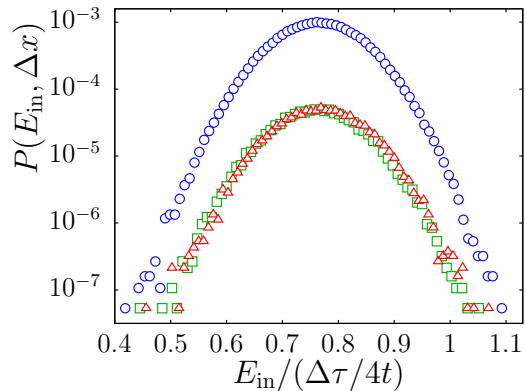


FIG. 13: (Color online) Probability distribution of the input energy gained by a single particle at fixed value of the shift of this particle, within the time lag  $\Delta\tau = 400t$  (i. e. 100 periods). The fixed shift is  $\Delta x = 282$  ( $\circ$ ),  $\Delta x = 283$  ( $\square$ ), and  $\Delta x = 284$  ( $\triangle$ ). The other parameters are  $N = L = 1200$ ,  $T = 10$ ,  $t = 16$ ,  $g = 0.1$ , and  $F = 0.1$ . The horizontal axis is normalized by the number of time periods, which is  $\Delta\tau/4t$ , therefore it expresses the energy input per period.

concentrated at them. But it is the minimum of the potential which is shifted above in the time evolution of the potential, so it is the particle at the minimum that acquires the energy from the source of the driving. Less particles at the minimum equals less input of energy, more precisely lowering of the positive part of the input energy. Conversely, the particles pushed off the instantaneous minima of the potential are found at the maxima of the potential. But these particles suffer lowering of the time-dependent potential, i. e. returning the energy back to the external source, therefore lowering also the negative part of the input energy. These two effects, i. e. unchanged current and lowered energy input, are the explanation of the increased efficiency. Of course, more subtle effects are also at work here. Especially, also the negative part of the energy input contributes. More importantly, if the interaction is strong enough, it changes the potential the particles move in to such extent that the current diminishes. At very small temperature, the current is sensitive to tiny changes in the shape of the potential and small changes in the interaction strength can cause big jumps in the current. We have seen these jumps in Fig. 3.

In addition to the averages, we measured also the full joint distribution function of particle shift and input energy (8). Because the work performed by one particle is proportional to its shift, we have in fact the joint distribution of performed work and input energy. As a first piece of information we plot in Fig. 12 the average energy input at fixed value of the particle shift, during the time interval  $\Delta\tau$ . We can observe the already discussed fact that interaction decreases the energy input. Here we can see that it holds also for most values of the shift, i. e. work performed by one single particle, separately.

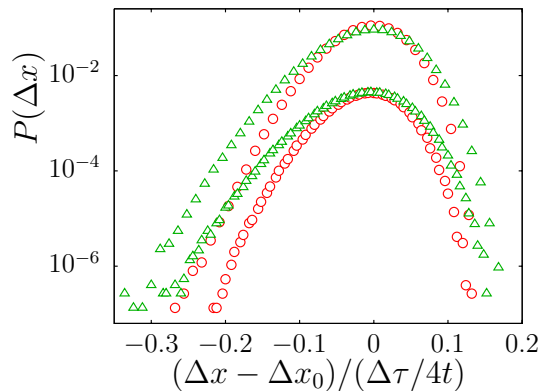


FIG. 14: (Color online) Probability distribution of the shift of a particle within the time lag  $\Delta\tau = 1000t$  (i. e. 250 periods), relative to the most probable value  $\Delta x_0$ . The interaction strength is  $g = 0$  (O, with  $\Delta x_0 = 718$ ) and  $g = 0.1$  ( $\Delta$ , with  $\Delta x_0 = 718$ ). The other parameters are  $N = L = 1200$ ,  $T = 10$ ,  $t = 16$ , and  $F = 0.1$ . The horizontal axis is normalized by the number of time periods, which is  $\Delta\tau/4t$ , therefore it expresses the shift per period.

The probability distribution of the energy input at fixed shift is shown in Fig. 13. We can see that the shape is pretty close to a Gaussian. This is far from being true for the distribution of the shift, which is proportional to the work performed by a single particle, as shown in Fig. 14. The distribution is skewed; when we compare the shifts shorter and longer than the most probable value, we find that the shorter are significantly more probable than the longer ones. This is due to the far-from-equilibrium character of the process. We can also see that the distribution is composed of two separate branches. The first one, with higher probability, corresponds to shifts which are multiples of 3, the period of the potential. The other shifts have significantly lower probability. In fact, it comes as no big surprise, that after integer number of time periods the particles like to be shifted by integer number of spatial periods.

The most important finding, however, stems from the comparison of the distribution in the case with and without interaction. In Fig. 14 we make this comparison for such set of parameters where we know that the interacting case exhibits higher efficiency. By analogy with equilibrium statistical physics one might be tempted to guess that higher efficiency is accompanied, or even caused, by milder fluctuations. The opposite holds in our model of the molecular motor. The fluctuations of the work performed by a single particle are higher in the interacting case. Therefore, we conclude that the increase of efficiency is not accompanied by decrease of fluctuations. On the contrary, the study of the energy balance discussed above together with the fact of increased fluctuations shows that the enhancement of efficiency is purely an energy effect.

## V. CONCLUSIONS

Interacting molecular motors moving in the power-stroke regime were modeled using a “reversible ratchet” model. Tunable on-site repulsive interaction leads to a host of intricate phenomena. The most important of them is the increase of energetic efficiency for small to moderate values of the interaction strength. We traced the origin of this effect to energy balance of the process. When the interaction is increased from zero, the performed work remains practically unchanged, while the input energy decreases. At the same time, the fluctuations of the performed work increase. This implies that the enhanced efficiency does not originate from the suppression of fluctuations, contrary to the situation in equilibrium heat machines.

Moreover, we observed that at very low temperature the dependence of current as well as efficiency on the interaction strength is rather complex, composed of many upward and downward steps. Hence, the efficiency has several, rather than single, local maxima as a function of interaction. As for the current, for suitable values of the parameters we can observe a sequence of current reversals when we increase the interaction strength. This complicated behavior is due to the interplay between size of steps in the external periodic potential, in which a particle moves, and the size of additional contributions to the potential from the interaction with other particles. However, this complicated dependence gradually disappears when the temperature increases. But the effect of current reversal due to interaction remains still visible.

We also investigated the response function of the current with respect to external load, both for zero load and for zero current. We showed that these two response functions differ substantially at zero or small interaction, but become identical when the interaction is large. We also revealed the structure with several peaks for both density and interaction dependence of the response function. Detailed study of the location of these maxima and minima showed that they correspond to specific fractional values of density and interaction. For example, the response is zero if the density is integer number and has maximum for densities equal to integer number of thirds, except the values which are themselves integers. In the interaction dependence, the peaks were found close to interaction strength equal to one half, one third and one fourth. We speculate that these special values are due to the fact that in those cases just one, two, and three particles on the same site, respectively, contribute to the potential by the value exactly equal to the amplitude of the external periodic potential. Contrary to the complicated step structure in the current, the peak structure in the response function survives also at higher temperatures.

The probability distribution of performed work and input energy reveals that the interaction leads to the increase of fluctuations, as we already mentioned. But we can see more. First, the distribution of work is far from

Gaussian. It is skewed so that the lower particle shift (i. e. work performed by an individual particle) relative to the maximum is more probable. This is the sign of far-from-equilibrium regime of the transport in the molecular motor. On the other hand, the input energy is Gaussian-distributed, when observed at fixed work.

There is also a very interesting principal question related to large-deviation properties of the fluctuation of the performed work. We made some simulations in this direction, which show that the work distribution, when properly rescaled, converges to a large-deviation function. In the last decade, there was a great surge of activity in the field of Fluctuation Theorems [74–84] but in our case the problem of applying these results lies in the choice of the proper quantity which would be both physically meaningful (or at least the physical meaning must not be enormously intricate) and satisfy the Fluctuation Theorem in some of the forms known so far. This question remains open.

Finally, we must also admit several drawbacks of our model, which can be lifted only by setting up a completely different scheme of particle movement. The first point is that the potential changes synchronously at all sites. This is unrealistic in biological motors, where each molecule has its internal “clock” telling in what phase of the chemical cycle the motor finds itself. It could be eas-

ily possible to simulate an asynchronous version of the algorithm. On the other hand, in technological applications the synchronicity in the potential changes may be built in into the system. The second point concerns the tunable interaction used in our model. Motor proteins interact always by steric hard-core repulsion and the effective weak repulsion may occur only as projection of real three-dimensional situation onto one-dimensional effective model [85, 86]. However, there is no principal obstacle to simulate three-dimensional case directly, if only sufficient computer power is available. Another way out is to generalize the asymmetric exclusion process in such a way that the maximum number of particles one site may accommodate is not one, but two, or three, etc. Simulations in this direction are under way.

### Acknowledgments

I gladly acknowledge inspiring discussions with P. Chvosta, E. Ben-Jacob and P. Kalinay. This work was carried out within the project AVOZ10100520 of the Academy of Sciences of the Czech republic and was supported by the Grant Agency of the Czech Republic, grant No. 202/07/0404.

- 
- [1] M. Schliwa (Ed.), *Molecular Motors* (Wiley-VCH, New York, 2003).
- [2] F. Jülicher, A. Ajdari, and J. Prost, *Rev. Mod. Phys.* **69**, 1269 (1997).
- [3] R. D. Astumian, *Science* **276**, 917 (1997).
- [4] P. Reimann and P. Hänggi, *Appl. Phys. A* **75**, 169 (2002).
- [5] P. Reimann, *Phys. Rep.* **361**, 57 (2002).
- [6] M. Schliwa and G. Woehlke, *Nature* **422**, 759 (2003).
- [7] P. Hänggi, F. Marchesoni, and F. Nori, *Ann. Phys. (Leipzig)* **14**, 51 (2005).
- [8] R. Lipowsky, Y. Chai, S. Klumpp, S. Liepelt, M. J. I. Müller, *Physica A* **372**, 34 (2006).
- [9] A. B. Kolomeisky and M. E. Fisher, *Annu. Rev. Phys. Chem.* **58**, 675 (2007).
- [10] H. Wang and T. C. Elston, *J. Stat. Phys.* **128**, 35 (2007).
- [11] K. Svoboda and S. M. Block, *Cell* **77**, 773 (1994).
- [12] H. Wang and G. Oster, *Nature* **396**, 279 (1998).
- [13] R. D. Astumian and M. Bier, *Biophys. J.* **70**, 637 (1996).
- [14] N. J. Carter and R. A. Cross, *Nature* **435**, 308 (2005).
- [15] U. Scheer, B. Xia, H. Merkert, and D. Weisenberger, *Chromosoma* **105**, 470 (1997).
- [16] I. Raška, K. Koberna, J. Malínský, H. Fidlerová, and M. Mašata, *Biology of the Cell* **96**, 579 (2004).
- [17] P. De Los Rios, A. Ben-Zvi, O. Slutsky, A. Azem, and P. Golubinoﬀ, *Proc. Natl. Acad. Sci. USA* **103**, 6166 (2006).
- [18] P. Hänggi and F. Marchesoni, *Rev. Mod. Phys.* **81**, 387 (2009).
- [19] S. Matthias and F. Müller, *Nature* **424**, 53 (2003).
- [20] C. Kettner, P. Reimann, P. Hänggi, and F. Müller, *Phys. Rev. E* **61**, 312 (2000).
- [21] H. Linke, T. E. Humphrey, A. Löfgren, A. O. Sushkov, R. Newbury, R. P. Taylor, and P. Omling, *Science* **286**, 2314 (1999).
- [22] R. A. Blythe and M. R. Evans, *J. Phys. A: Math. Theor.* **40**, R333 (2007).
- [23] A. Ajdari and J. Prost, *C. R. Acad. Sci. Paris, Série II* **315**, 1635 (1992).
- [24] M. O. Magnasco, *Phys. Rev. Lett.* **71**, 1477 (1993).
- [25] R. Bartussek, P. Hänggi, and J. G. Kissner, *Europhys. Lett.* **28**, 459 (1994).
- [26] A. B. Kolomeisky and B. Widom, *J. Stat. Phys.* **93**, 633 (1998).
- [27] H. Qian, *Biophys. Chem.* **67**, 263 (1997).
- [28] H. Qian, *Biophys. Chem.* **83**, 35 (2000).
- [29] H. Qian, *Phys. Rev. E* **69**, 012901 (2004).
- [30] C. Maes and M. H. van Wieren, *J. Stat. Phys.* **112**, 329 (2003).
- [31] A. B. Kolomeisky, E. B. Stukalin, and A. A. Popov, *Phys. Rev. E* **71**, 031902 (2005).
- [32] Z. Wang, M. Feng, W. Zheng, and D. Fan, *Biophys. J.* **93**, 3363 (2007).
- [33] R. Lipowsky and S. Liepelt, *J. Stat. Phys.* **130**, 39 (2008).
- [34] R. K. Das and A. B. Kolomeisky, *Phys. Rev. E* **77**, 061912 (2008).
- [35] A. Vilfan, *Frontiers in Bioscience* **14**, 2269 (2009).
- [36] H. Wang and G. Oster, *Europhys. Lett.* **57**, 134 (2002).
- [37] F. Jülicher and J. Prost, *Phys. Rev. Lett.* **75**, 2618 (1995).
- [38] K. Sekimoto, cond-mat/9611005.
- [39] K. Sekimoto, *J. Phys. Soc. Japan* **66**, 1234 (1997).
- [40] H. Kamegawa, T. Hondou, and F. Takagi, *Phys. Rev. Lett.* **80**, 5251 (1998).

- [41] J. M. R. Parrondo and B. J. De Cisneros, *Appl. Phys. A* **75**, 179 (2002).
- [42] M. Asfaw and M. Bekele, *Phys. Rev. E* **72**, 056109 (2005).
- [43] J. M. R. Parrondo, J. M. Planco, J. F. Cao, and R. Brito, *Europhys. Lett.* **43**, 248 (1998).
- [44] H. Wang and G. Oster, *Appl. Phys. A* **75**, 315 (2002).
- [45] J. M. R. Parrondo, *Phys. Rev. E* **57**, 7297 (1998).
- [46] R. D. Astumian and I. Derényi, *Biophys. J.* **77**, 993 (1999).
- [47] A. Parmeggiani, F. Jülicher, A. Ajdari, and J. Prost, *Phys. Rev. E* **60**, 2127 (1999).
- [48] T. Schmiedl and U. Seifert, *Europhys. Lett.* **83**, 30005 (2008).
- [49] C. T. MacDonald, J. H. Gibbs, and A. C. Pipkin, *Biopolymers* **6**, 1 (1968).
- [50] C. T. MacDonald and J. H. Gibbs, *Biopolymers* **7**, 707 (1969).
- [51] B. Derrida, E. Domany, and D. Mukamel, *J. Stat. Phys.* **69**, 667 (1992).
- [52] B. Derrida, M.R. Evans, V. Hakim and V. Pasquier, *J. Phys. A: Math. Gen.* **26**, 1493 (1993).
- [53] B. Derrida, *Phys. Rep.* **301**, 65 (1998).
- [54] A. Parmeggiani, T. Franosch, and E. Frey, *Phys. Rev. Lett.* **90**, 086601 (2003).
- [55] A. Parmeggiani, T. Franosch, and E. Frey, *Phys. Rev. E* **70**, 046101 (2004).
- [56] P. Greulich, A. Garai, K. Nishinari, A. Schadschneider, and D. Chowdhury, *Phys. Rev. E* **75**, 041905 (2007).
- [57] A. Basu and D. Chowdhury, *Phys. Rev. E* **75**, 021902 (2007).
- [58] T. Tripathi and D. Chowdhury, *Phys. Rev. E* **77**, 011921 (2008).
- [59] K. Nagel and M. Schreckenberg, *J. Phys. I France* **2**, 2221 (1992).
- [60] R. Lipowsky, S. Klumpp, and T. M. Nieuwenhuizen, *Phys. Rev. Lett.* **87**, 108101 (2001).
- [61] S. Klumpp and R. Lipowsky, *Proc. Natl. Acad. Sci. USA* **102**, 17284 (2005).
- [62] I. Derényi and T. Vicsek, *Phys. Rev. Lett.* **75**, 374 (1995).
- [63] I. Derényi and A. Ajdari, *Phys. Rev. E* **54**, R5 (1996).
- [64] Y. Aghababaie, G. I. Menon, and M. Plischke, *Phys. Rev. E* **59**, 2578 (1999).
- [65] P. Reimann, R. Kawai, C. van den Broeck, and P. Hänggi, *Europhys. Lett.* **45**, 545 (1999).
- [66] E. B. Stukalin, H. Phillips III, and A. B. Kolomeisky, *Phys. Rev. Lett.* **94**, 238101 (2005).
- [67] E. B. Stukalin and A. B. Kolomeisky, *Phys. Rev. E* **73**, 031922 (2006).
- [68] O. Campàs, Y. Kafri, K. B. Zeldovich, J. Casademunt, and J.-F. Joanny, *Phys. Rev. Lett.* **97**, 038101 (2006).
- [69] F. Jülicher and J. Prost, *Phys. Rev. Lett.* **78**, 4510 (1997).
- [70] M. Badoual, F. Jülicher, and J. Prost, *Proc. Natl. Acad. Sci. USA* **99**, 6696 (2002).
- [71] M. N. Artyomov, A. Yu. Morozov, and A. B. Kolomeisky, *Phys. Rev. E* **77**, 040901(R) (2008).
- [72] F. Slanina, *Europhys. Lett.* **84**, 50009 (2008).
- [73] F. Slanina, *J. Stat. Phys.* **135**, 935 (2009).
- [74] D. J. Evans, E. G. D. Cohen, and G. P. Morriss, *Phys. Rev. Lett.* **71**, 2401 (1993).
- [75] G. Gallavotti and E. G. D. Cohen, *Phys. Rev. Lett.* **74**, 2694 (1995).
- [76] J. Kurchan, *J. Phys. A: Math. Gen.* **31**, 3719 (1998).
- [77] J. L. Lebowitz and H. Spohn, *J. Stat. Phys.* **95**, 333 (1999).
- [78] C. Maes and K. Netočný, *J. Stat. Phys.* **110**, 269 (2003).
- [79] U. Seifert, *Europhys. Lett.* **70**, 36 (2005).
- [80] D. Andrieux and P. Gaspard, *Phys. Rev. E* **74**, 011906 (2006).
- [81] A. W. C. Lau, D. Lacoste, and K. Mallick, *Phys. Rev. Lett.* **99**, 158102 (2007).
- [82] R. D. Astumian, *Phys. Rev. E* **76**, 020102(R) (2007).
- [83] R. J. Harris and G. M. Schütz, *J. Stat. Mech.* P07020 (2007).
- [84] E. Šubrt and P. Chvosta, *J. Stat. Mech.* P09019 (2007).
- [85] P. Kalinay and J. K. Percus, *J. Chem. Phys.* **122**, 204701 (2005).
- [86] P. Kalinay and J. K. Percus, *Phys. Rev. E* **74**, 041203 (2006).